

Visible and near-infrared dual band switchable metasurface edge imaging: supplement

GUANGHAO CHEN,^{1,†} JUNXIAO ZHOU,^{1,†} STEVEN EDWARD BOPP,²
JUNXIANG ZHAO,¹ AND ZHAOWEI LIU^{1,2,*}

¹*Department of Electrical and Computer Engineering, University of California, San Diego, La Jolla, California 92093, USA*

²*Materials Science and Engineering Program, University of California, San Diego, La Jolla, California 92093, USA*

*Corresponding author: z4liu@eng.ucsd.edu

[†]These authors contributed equally to this work

This supplement published with Optica Publishing Group on 4 August 2022 by The Authors under the terms of the [Creative Commons Attribution 4.0 License](https://creativecommons.org/licenses/by/4.0/) in the format provided by the authors and unedited. Further distribution of this work must maintain attribution to the author(s) and the published article's title, journal citation, and DOI.

Supplement DOI: <https://doi.org/10.6084/m9.figshare.20343267>

Parent Article DOI: <https://doi.org/10.1364/OL.465128>

Visible and near-infrared dual band switchable metasurface edge imaging: supplemental document

1. Impact of nanostructure volume shrinkage on the device

Sb₂S₃ alloys, like many other phase change materials, experiences volume contraction after being switched to its crystalline state. The volume of Sb₂S₃ contracts as crystallization occurs. So far, we haven't seen experimental data quantifying the amount of contraction. Hence, we will use the result from a similar phase change material, GST, which displays about 7% density increment at crystalline state [1, 2], to produce a rough estimate.

In our design, since all the structures are buried in the silica, we assumed all change occurs to the height. It will shrink to around 465 nm at **Function 2** when all Sb₂S₃ is switched to the crystalline state. We included this effect in our simulation to test the impact to the device performance. The result (Fig. S1) shows that the A2 array indeed benefits from this volume shrinkage. The transmission increases from 73% to 77%, while that of the 575 nm does not have noticeable change.

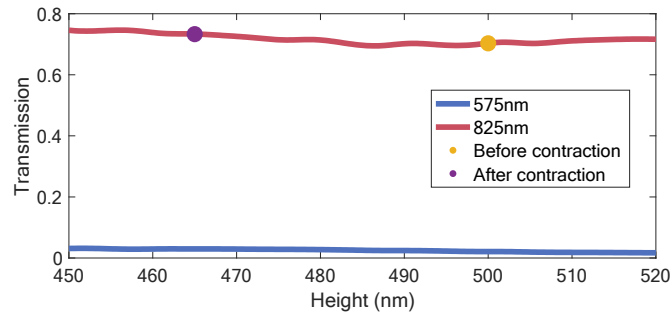


Fig. S1 Transmission of A2 array at 575 nm and 825 nm.

2. Geometrical phase delay introduced by the rotated nanobars

Figure. S2 shows the phase responses of the A1 and A2 arrays at their corresponding working states. The simulation is carried out in COMSOL by monitoring the forward scattering phase delay of the orthogonal polarization as it sweeps the incident wavelength and the nanobar rotation angle. In data processing, since dispersion is not the primary interest in this study, the phase functions are only unwrapped along the horizontal axis and then aligned at 0° rotation angle for easier data comparison. Figure. S2 (a) is the phase responses of A1 array at amorphous Sb₂S₃. The wavelength covers 500-750 nm, which is the transmission window of this array. Similarly, the phase responses of A2 at crystalline Sb₂S₃ is shown in Fig. S2 (b).

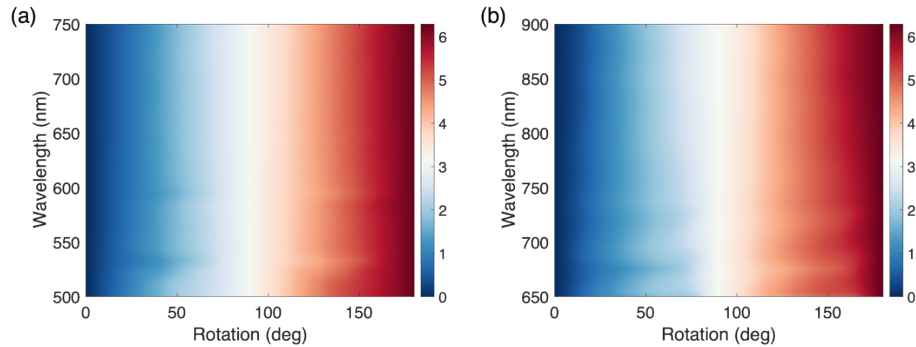


Fig. S2 (a) Phase responses from A1 array at amorphous Sb_2S_3 . (b) Phase responses from A2 array at crystalline Sb_2S_3 . The phase functions are only unwrapped along the rotation angle axis. Phase functions of all wavelengths are aligned at 0° rotation angle for comparison.

The phase response of either array increases from 0 to 2π monotonically as rotation angle sweeps from 0 to 180° .

3. Imaging simulation with angular spectrum method

Results of the image simulation in the main text (Fig. 3 and Fig. 4) are generated with angular spectrum method [3]. The scalar diffraction process of a field from the aperture plane to the destination plane is by filtering the angular spectrum (in the Fourier domain) with a free-space transfer function, $\exp\left[i\frac{2\pi}{\lambda}z(1 - \alpha^2 - \beta^2)\right]$, where α and β are the directional cosines. The input and the output of the propagation should both be complex functions in the real space. Thus, Fourier transform and inverse Fourier transform are both needed for one beam propagation. Since we use a $4f$ system, the full beam propagation process is: 1) beam propagation from the source to the lens. 2) Multiplication with the lens pupil function. 3) Beam propagation from the lens to the metasurface. 4) Multiplication with the metasurface pupil function. 5) Beam propagation from the metasurface to the lens. 6) Multiplication with the lens pupil function. 7) Beam propagation from the lens to the image plane. Only the intensity is measured on this plane. The polarization conversion, however, is not explicitly modeled in this simulation, since interference only occurs for fields of the same polarization.

References

1. M. N. Julian, C. Williams, S. Borg, S. Bartram, and H. J. Kim, *Optica* 7, 746-754 (2020).
2. G. D'Arrigo, M. Scuderi, A. Mio, G. Favarò, M. Conte, A. Sciuto, M. Buscema, G. Li-Destri, E. Carria, D. Mello, M. Calabretta, A. Sitta, J. Pries, and E. Rimini, *Mater. Des.* 202, 109545 (2021).
3. J. W. Goodman, *Introduction to fourier optics* (Roberts and Company Publishers, 2005).